IEICE TRANS. FUNDAMENTALS, VOL.E82–A, NO.8 AUGUST 1999

PAPER *Special Section on Digital Signal Processing*

A Frequency Domain Adaptive Algorithm for Estimating Impulse Response with Flat Delay and Dispersive Response Region

Yoji YAMADA[†], **Hitoshi KIYA**[††], ***and*** **Noriyoshi KAMBAYASHI**[†††], ***Members***

SUMMARY In some applications, such as the echo cancellation problem of satellite-linked communication channels, there occurs a problem of estimation of a long impulse response, which consists of a long flat delay and a short dispersive response region. In this paper, it is shown that the use of the adaptive algorithm based on the frequency domain sampling theorem enables efficient identification of the long impulse response. The use of the proposed technique can lead to the reduction of both the number of adaptive weights and the complexity of flat delay estimation.

key words: *impulse response, delay, frequency domain, system identification, dispersive response region*

1. Introduction

In some adaptive filter applications, the unknown impulse response consists of several delays and short dispersive response regions [1]–[7]. In typical applications, such as echo path estimation of satellite-linked communication channels, the delay is as long as over 600 milliseconds, whereas the dispersive response region is only of the order of less than 10 milliseconds [7].

Figure 1 shows a model [5] of the impulse response of the echo path which has a long flat delay and a short dispersive response region. In the model, L, D and N represent the length of the impulse response, the length of the flat delay and the length of the dispersive region, respectively. The flat delay arises from the large propagation delay in the communication channels, and it increases the tap length of the adaptive filters.

To estimate the impulse response with the flat delay and dispersive response region, several time domain adaptation algorithms have been studied. The STWQ (scrub taps waiting in a queue) [4] and the SELQUE (select and queue with a constraint) [5]–[7] algorithms enable efficient reduction of the number of adaptive coefficients by utilizing a sparse tap adaptive finite impulse response (FIR) filter, as shown in Fig. 2.

Although the STWQ and SELQUE algorithms decrease the number of adaptive coefficients, the delay estimation algorithm and the impulse response identification algorithm cannot be separated. If the flat delay changes, these algorithms must restart their tap allocation and adaptation processes from the initial state.

In this paper, we propose the use of the frequency domain adaptive algorithm [8] based on the frequency domain sampling theorem [9]. Since the proposed technique evaluates the subband signals in equally spaced discrete frequency points regardless of the length of the flat delay D, it can lead to the reduction of both the number of adaptive weights and the complexity of the flat delay estimation. In addition, the flat delay estimation and the impulse response estimation of the dispersive region can be performed independently.

In the following section, the problem is defined. Section 3 describes the proposed frequency domain algorithm. In Sect. 4, the impulse response identification algorithm of the dispersive region and flat delay esti-

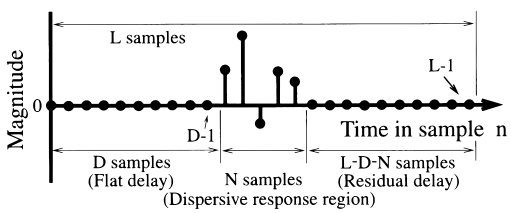

Fig. 1 A model of the impulse response with flat delay and dispersive region.

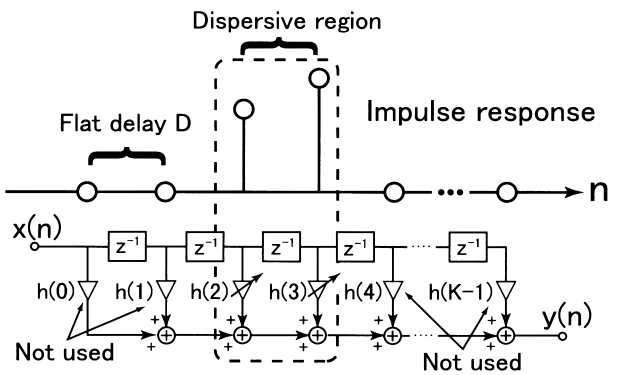

Fig. 2 Conventional time domain adaptation scheme for the impulse response with flat delay D.

Manuscript received December 7, 1998.
Manuscript revised March 10, 1999.

[†]The author is with the Ishikawa National College of Technology, Ishikawa-ken, 929-0392 Japan.
[††]The author is with the Department of Electrical Engineering, Graduate School of Tokyo Metropolitan University, Hachioji-shi, 192-0397 Japan.
[†††]The author is with the Faculty of Engineering, Nagaoka University of Technology, Nagaoka-shi, 940-2188 Japan.

mation problem are considered. Section 5 is a discussion of the arithmetic complexity. Finally, in Sect. 6, simulation results are provided, which confirm the effectiveness of the proposed method.

2. Problem Definition

Let us define the model of the unknown impulse response [5] with total length L, as shown in Fig. 1. The model consists of a flat delay of length D, a dispersive response region of length N and residual delay $L - D - N$. In the model, z^{-D} represents the flat delay and an actual delay T_D[sec] is given by $T_D = D \times T_s$[sec], where T_s[sec] represent sampling interval.

In typical applications, such as echo path estimation problems of satellite-linked communication channels, it is well known that $L, D \gg N$. The flat delay D and the total length L depend on the propagation delay in communication channels and the dispersive response region corresponds to the model of an echo from a hybrid.

In this paper, let us assume the following conditions.

(a) The lengths L and N are unknown, while the upper bounds of L and N are given.
(b) $L > N$ is satisfied.
(c) The length D is unknown *a priori*.
(d) The position of the flat delay region and the dispersive region are unknown *a priori*.
(e) The energy of the samples which corresponds to the flat delay region and the residual delay region is negligibly small.

3. Frequency Domain Adaptive Algorithm Based on the Frequency Domain Sampling Theorem

3.1 Frequency Domain Sampling Theorem

First, we consider the frequency domain sampling theorem [9]. For simplicity, we use the notation $F(\omega)$ instead of the notation $F(e^{j\omega})$.

[Frequency domain sampling theorem] Let $F(\omega)$ be the discrete time Fourier transform (DTFT) of a finite duration discrete sequence $f(n)$, $(0 \le n \le N-1)$. We denote this relationship as

$$f(n) \overset{\text{DTFT}}{\leftrightarrow} F(\omega). \tag{1}$$

The frequency domain sample $F(\omega_k)$ is defined as

$$F(\omega_k) = F(\omega)|_{\omega=\frac{2\pi k}{M}} \quad (k = 0, 1, \cdots, M-1). \tag{2}$$

If the condition $M \ge N$ is satisfied, the discrete sequence $f(n)$ can be perfectly determined from the inverse discrete Fourier transform (IDFT) of $F(\omega_k)$.

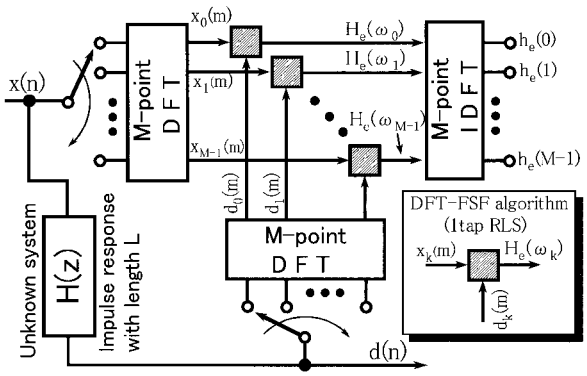

Fig. 3 Implementation of the frequency domain adaptive system identification block diagram utilizing the DFT-FSF banks.

Note that, in the above theorem, $F(\omega)$ denotes a continuous spectrum, whereas $F(\omega_k)$ denotes a line spectrum.

3.2 Frequency Domain Identification Utilizing the DFT-FSF Banks

Let us consider frequency domain system identification methods [8],[10]–[12], which utilize the DFT frequency sampling filter (DFT-FSF) banks. The DFT-FSF bank is a family of the alias-free frequency sampling filter (FSF) bank [13],[14] and these filter banks have alias-free properties at equally spaced discrete frequency points.

Figure 3 shows the M subband implementation of the adaptive system identification block diagram, based on the frequency domain sampling theorem, and Table 1 shows the DFT-FSF adaptive algorithm [8]. The limiting value analysis of the algorithm is considered in [11].

$H(z)$ denotes an unknown system and $\boldsymbol{h}$ represents its impulse response of length L. $H(\omega)$ is the frequency response of $H(z)$. $x(n)$ and $d(n)$ represent the input and desired signals, respectively. The unknown impulse response $\boldsymbol{h}$ can be expressed as

$$\boldsymbol{h} = [h(0), h(1), \cdots, h(L-1)]. \tag{3}$$

$H(\omega_k)$, $(\omega_k = \frac{2\pi k}{M}, k = 0, 1, \cdot\cdot, M-1)$ denotes the frequency domain samples of the unknown system, while $H_e(\omega_k)$ denotes the estimation of $H(\omega_k)$. By applying the frequency domain identification algorithm, as shown in Table 1, we can obtain $H_e(\omega_k)$.

If the condition $M \ge L$ is satisfied, the estimated unknown impulse response $\boldsymbol{h_e}$ can be obtained from the IDFT of $H_e(\omega_k)$ based on the frequency domain sampling theorem. The estimated unknown impulse response $\boldsymbol{h_e}$ can be expressed as

$$\boldsymbol{h_e} = [h_e(0), h_e(1), \cdots, h_e(M-1)], \tag{4}$$

$$h_e(n) = \begin{cases} h(n) & 0 \le n \le L-1 \\ 0 & L \le n \le M-1. \end{cases} \tag{5}$$

Table 1 DFT-FSF adaptive algorithm using the frequency domain 1-tap adaptive weights.

m : time variable k : bank number
$for \quad k = 0 \quad to \quad M-1$
$\hat{x}_k(m) = \alpha \hat{x}_k(m-1) + x_k(m)$
$\hat{d}_k(m) = \alpha \hat{d}_k(m-1) + d_k(m)$
$r_k(m) = \lambda r_k(m-1) + \hat{x}_k(m)\hat{x}_k^*(m)$
$p_k(m) = \lambda p_k(m-1) + \hat{d}_k(m)\hat{x}_k^*(m)$
$H_e(\omega_k) = p_k(m)/r_k(m)$

* denotes complex conjugate.

Hence the DFT-FSF adaptive system has an M-channel bin and 1-tap adaptive weight in each bin; it corresponds to the M tap adaptive system in the time domain [8].

4. Impulse Response Identification of the Dispersive Region

The proposed algorithm can separate the impulse response identification algorithm and the flat delay estimation algorithm. In this section, we describe the identification algorithm to identify the impulse response of the dispersive response region defined in Fig. 1.

Figure 4 (a) represents the DTFT pair of the unknown impulse response $\boldsymbol{h}$ and its frequency domain representation $H(\omega)$. Figures 4 (b) and (c) represent the impulse response $\boldsymbol{h_e}$ which is obtained by the IDFT of the estimated frequency domain samples $H_e(\omega_k)$. The estimated impulse response $h_e(n)$ can be expressed as

$$h_e(n) = \frac{1}{M} \sum_{k=0}^{M-1} H_e(\omega_k) e^{j\frac{2\pi nk}{M}}, \quad (0 \le n \le M-1). \tag{6}$$

Our goal is to estimate the impulse response of the dispersive response region using only $M(M > N)$ adaptive weights in the frequency domain. Let us consider the following two cases of $M \ge L$ and $L > M \ge N$, as shown in Figs. 4 (b) and (c).

4.1 Redundancy of the Estimated Impulse Response

In this section, we assume that the condition $M \ge L$ is satisfied. Figure 4 (b) shows an example in the case of $L = 7$ and $M = 8$. In this case, the frequency domain sampling theorem is satisfied. Therefore, from Eq. (6), we can obtain the entire unknown impulse response $\boldsymbol{h_e}$ as a discrete sequence with period M shown in Eq. (4).

In addition, the obtained impulse response $\boldsymbol{h_e}$ has redundant zeros, as shown in the next equation.

$$h_e(n) \simeq \begin{cases} 0 & 0 \le n \le D-1 \quad (7a) \\ 0 & D+N \le n \le M-1 \quad (7b) \end{cases}$$

Equation (7a) deals with the flat delay D and Eq. (7b) deals with the redundancy of the DFT of size M.

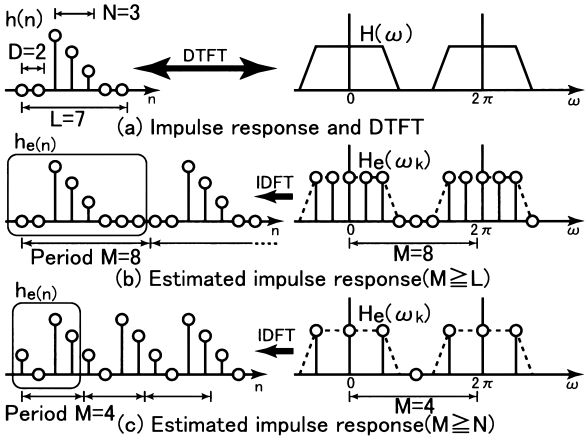

Fig. 4 The time domain and the frequency domain representation of the estimated impulse response of the dispersive response region.

4.2 Proposed Estimation Method

In this section, we assume that the condition $L > M \ge N$ is satisfied. Figure 4 (c) shows an example for the case of $L = 7$ and $M = 4$. In this case, for the condition $M < L$, the frequency domain sampling theorem is not satisfied. Usually, this leads to time domain aliasing in the obtained impulse response $\boldsymbol{h_e}$. However, the obtained sequence $\boldsymbol{h_e}$ is not disturbed by the time domain aliasing.

The reason for this is as follows.

(A) The proposed algorithm identify the unknown system at the alias-free discrete frequencies based on the frequency domain sampling theorem.

(B) From the definition, the unknown impulse response has only N non zero samples and the other samples are negligibly small.

(C) $\boldsymbol{h_e}$ is determined as the discrete sequence with period M, where $M > N$ is satisfied.

Since the time domain aliasing arises only in the region represented by Eqs. (7a) and (7b), the obtained sequence $\boldsymbol{h_e}$ not disturbed by the time domain aliasing.

However, due to the influence of the flat delay D, an extra phase shift term arises in the estimated frequency domain samples $H_e(\omega_k)$. As a result, the relationship in Eq. (5) is not satisfied.

Let us consider the obtained impulse response $h_e(n)$ and the extended version of the periodic sequence $\tilde{h}_e(n)$, as shown in Fig. 5. The relationship between $h_e(n)$ and $\tilde{h}_e(n)$ is described as

$$\tilde{h}_e(n) = \begin{cases} h_e(n) & 0 \le n \le M-1 \\ \tilde{h}_e(n-M) & \text{otherwise.} \end{cases} \tag{8}$$

Let us denote the true estimated impulse response

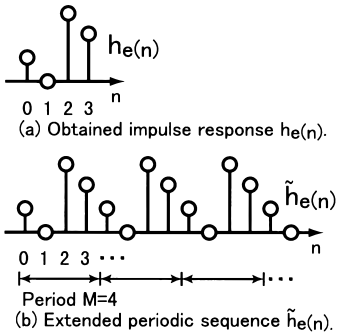

Fig. 5 The obtained impulse response $h_e(n)$ and extended periodic sequence $\tilde{h}_e(n)$.

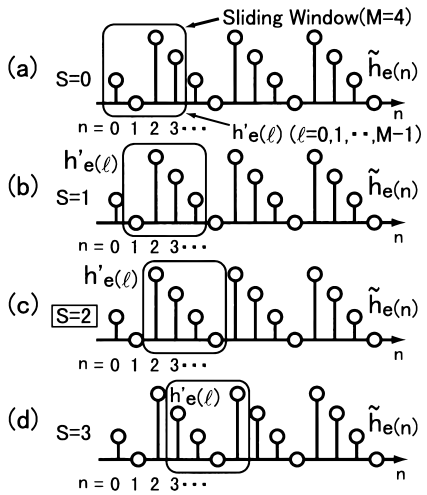

Fig. 6 An example of the candidates of the true estimated impulse response $h'_e(\ell)$,$(L = 7, D = 2, N = 3, M = 4)$.

of the dispersive region as

$$\boldsymbol{h'_e} = [h'_e(0), h'_e(1), \cdots, h'_e(M-1)]. \tag{9}$$

In Fig. 6, the candidates of the true estimated impulse response $h'_e(\ell)(\ell = 0, 1, \cdots, M-1)$, which correspond to the dispersive region of the unknown impulse response, are depicted in the case of $M = 4$. Obviously, since $\tilde{h}_e(n)$ is a periodic sequence with period M, there are only M independent candidates, as shown in Fig. 6 (a) to (d). The relationship between the candidates $h'_e(\ell)$ and $\tilde{h}_e(n)$ is described as

$$h'_e(\ell) = \tilde{h}_e(\ell + S), \quad (0 \le \ell \le M-1). \tag{10}$$

where S $(0 \le S \le M-1)$ is defined as the shift value.

On the other hand, from the conditions (A), (B) and (C) described in Sect. 4.2, $\boldsymbol{h'_e}$ should have redundant nearly zero components in the tail. The length of zero components is $M - N$. Thus, the true estimated impulse response $\boldsymbol{h'_e}$ should have the following form.

$$\boldsymbol{h'_e} = [h'_e(0), h'_e(1), \cdots, h'_e(N-1), \underbrace{0, \cdots, 0}_{M-N}] \tag{11}$$

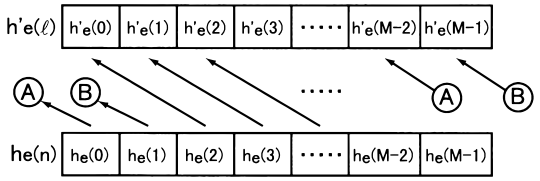

Fig. 7 The circular rotation representation of the obtained impulse response (in the case of $S = 2$).

From Eqs. (10) and (11), we can choose the correct impulse response of the dispersive region by selection from the M candidates of $\boldsymbol{h'_e}$.

The above considerations are summarized as follows.

[Estimation procedure of $\boldsymbol{h'_e}$]

step1 To obtain $\boldsymbol{h_e}$, running the algorithm which described in Table 1 and calculate Eq. (6).

step2 Define the periodic sequence $\tilde{h}_e(n)$ as shown in Eq. (8).

step3 By using of the sliding window with length M, as shown in Fig. 6, extract M candidates of $\boldsymbol{h'_e}$ in the case of $S = 0$ to $S = M - 1$.

step4 Choose a $\boldsymbol{h'_e}$ which satisfies Eq. (11) from the selection of the above candidates.

step5 Record the value of S which correspond to the selected candidate. S will be use an estimation of the flat delay.

In the above procedure, a condition $M > N$ is required. From the definition, the length of N is unknown while the upper bound of N is given, therefore we can choose M to satisfy the necessary condition $M > N$. In Fig. 6 (c), an example of the selected candidate using the above procedure with $S = 2$ in the case of $M = 4$, $N = 3$ is given.

To represent the relationship between $h_e(n)$ and $h'_e(\ell)$, let us consider a circular rotation representation of $h_e(n)$ and $h'_e(\ell)$ as shown in Fig. 7. From Eqs. (8) and (10), the desired impulse response $h'_e(\ell)$ can be written as

$$h'_e(\ell) = \begin{cases} h_e(\ell + S) & 0 \le \ell \le M - S - 1 \\ h_e(\ell - M + S) & M - S \le \ell \le M - 1, \end{cases} \tag{12}$$

where

$$S = (\ (D)\ )_M = (D_{\mathrm{mod}} M). \tag{13}$$

In Eq. (13), $(D_{\mathrm{mod}} M)$ represents an operation to take the remainder after division of M. Note that, although S is given by Eq. (13), the above estimation procedure of $\boldsymbol{h'_e}$ should be used instead of Eq. (12) as D was assumed to be unknown.

The proposed technique only requires M $(M > N)$ adaptive weights in the frequency domain even in the case of the long impulse response with total length L and flat delay D.

4.3 Restriction of the Proposed Method

In the estimation procedure of $\boldsymbol{h'_e}$, which described in the previous section, the restriction of the value of $\boldsymbol{h'_e}$ is not considered.

In Eq. (11), $h'_e(\ell)(0 \leq \ell \leq N-1)$ should not includes the zero vector of order greater than $M-N$. If this condition is not satisfied, the **step3** is not available.

To avoid this problem, one of the following conditions is required.

(a) Choose the DFT size as $M > N + O_z$. O_z represents the order of the zero vector in $h'_e(\ell)(0 \leq \ell \leq N-1)$.

(b) Choose the DFT size as $M > 2N$.

As a result, it increases an arithmetic complexity of the proposed method. However, the cost is not quite large under the condition $L \gg N$.

4.4 Estimation of the Flat Delay

From the previous discussion, the upper bound of D is given by $L-M$, while the flat dely D becomes a quantized value which is a multiple of M. From Eq. (13), the possible values of D can be expressed by

$$D = k \times M + S, \qquad 0 \leq k \leq \left\lceil \frac{L-M}{M} \right\rceil. \tag{14}$$

In Eq. (14), k represents an integer and the notation $\lceil \cdot \rceil$ represents the smallest integer which is not less than its argument.

There are k possibilities for determining the flat delay D. The selection of D can be done from observations of the residual error $e(n)$, using a convolution filter $V(z)$ with length $D+M$ as shown in Fig. 8. In Fig. 8, $x(n)$ and $y(n)$ represent the input signal and the echo reprica, respectively. $g(n)$ represents a model of additive noise. It is guaranteed that we can determine the flat delay D after the k-th trial.

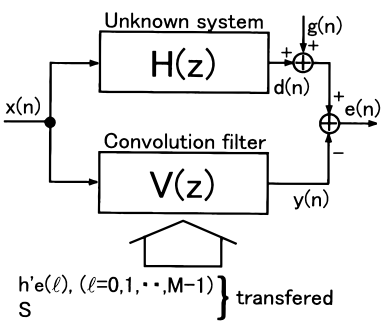

Fig. 8 Echo suppression scheme of the proposed method.

5. Discussion of the Complexity of the Implementation

In this section, let us consider the complexity involved in the implementation of the proposed technique. Table 2 summarizes the proposed technique and the conventional time domain algorithm for the following four items.

- L_{conv}: The length of the entire delay in the convolution filter.
- C_{tap}: The number of combinations of tap allocations in the delay estimation problem after D has changed.
- Q_{Len}: The length of the queue in the algorithm.
- O_c: The order of the arithmetic complexity of the adaptive filtering per a sample.

In Table 2, we assume that the number of adaptive coefficients is M.

Let us consider the number of combinations C_{tap} after D has changed. In the proposed technique, the flat delay estimation and the impulse response estimation are performed independently, thus the impulse response estimation accuracy is not disturbed by the changing of the flat delay D. As a results, if D changes, according to Eq. (14) C_{tap} becomes $\lceil \frac{L-M}{M} \rceil$ even in the worst case, as shown in Table 2.

In the STWQ and SELQUE, the flat delay estimation and the impulse response estimation algorithms are not separated. Thus, in this case, these algorithms should restart their flat delay estimation and tap update proceses from the initial state even if only D has changed. In the STWQ and SELQUE, C_{tap} is given by $L-N+1$, as shown in Table 2.

Figure 9 shows the comparison of the value of C_{tap} in the case of $N = 0.1L$ and $N = 0.01L$. We can significantly reduce the value of C_{tap} under the condition $L \gg N$ for large L.

In Table 2, the length Q_{Len} in the proposed algorithm represents the value of k in Eq. (14), while Q_{Len} for STWQ and SELQUE represents the total length of the waiting queue for active tap control. For the proposed method, O_c includes arithmetic complexity of the additional convolution filter as shown in Fig. 8.

Table 2 Complexity of implementation of algorithms.

	Proposed	STWQ [4]	SELQUE [6]
Length of delay:L_{conv}	L	L	L
Tap allocation:C_{tap}	$\lceil \frac{L-M}{M} \rceil$	$L-M+1$	$L-M+1$
Length of queue:Q_{Len}	$\lceil \frac{L-M}{M} \rceil$	$L-M$	$L-M$
Adaptive filtering:O_c	$O(\log_2 M + M)$ [8]	$2M$	$2M$

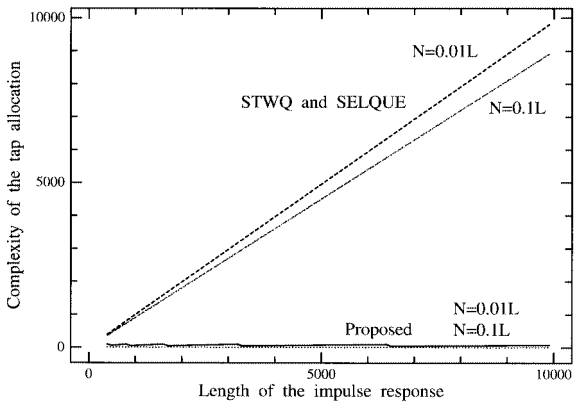

Fig. 9 Comparison of the complexity of tap re-allocation.

6. Simulation Example

In this section, by using the proposed method, the impulse response identification of the dispersive response region is demonstrated in a simulation example. Then, we will consider comparison of the mean square error (MSE) convergence property of the proposed method and the conventional time domain algorithm.

All simulation examples are done under the 32bit floating point operation.

6.1 IRER Convergence

[Conditions]

- Unknown system: $L = 53, D = 50, N = 3$.
- Dispersive region: $h(50) = 1, h(51) = 2$, $h(52) = -1$ (as shown in Fig. 10 (a)).
- DFT size: $M = 4$.
- Input signal: Gauss noise with variance $\sigma^2 = 1$, mean value $m = 0$.
- Forgetting constant: $\alpha = \lambda = 0.999$.

Figure 10 (a) shows the dispersive region of the unknown impulse response. Figures 10 (b) and (c) show the obtained impulse response $h_e(n)$ and the impulse response estimation ratio (IRER) convergence, respectively. The definition of the IRER is given by

$$\mathrm{IRER} = 10\log_{10}\frac{|\boldsymbol{h}-\boldsymbol{h}'_{\boldsymbol{e}}|^T|\boldsymbol{h}-\boldsymbol{h}'_{\boldsymbol{e}}|}{\boldsymbol{h}^T\boldsymbol{h}}. \tag{15}$$

In this example, by using of the estimation procedure of $\boldsymbol{h}'_{\boldsymbol{e}}$, we can obtain $S = 2$. The estimated impulse response $h'_e(\ell)$ are as follows in the case of IRER $= -49.0$ [dB].

$$\begin{aligned} h'_e(0) &= 9.997744560\mathrm{e}-01 \simeq h(50) \\ h'_e(1) &= 1.993155241\mathrm{e}+00 \simeq h(51) \\ h'_e(2) &= -9.947283268\mathrm{e}-01 \simeq h(52) \\ h'_e(3) &= 5.498528481\mathrm{e}-04 \simeq h(53) \end{aligned}$$

In addition, by substituting $S = 2$ into Eq. (12), we can confirm the relationship between $h'_e(\ell)$ and $h_e(n)$ as shown in Fig. 10 (b), where $h'_e(\ell)$ is a estimated dispersive response region of $h(n)$.

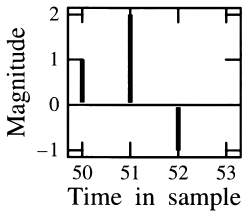

(a) Dispersive region of the unknown impulse response $h(n)$ with the total length $L = 53$.

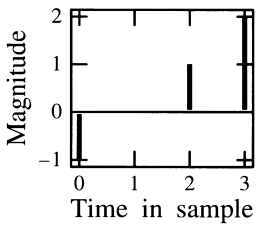

(b) Obtained impulse response $h_e(n)$ $(M = 4, S = 2)$.

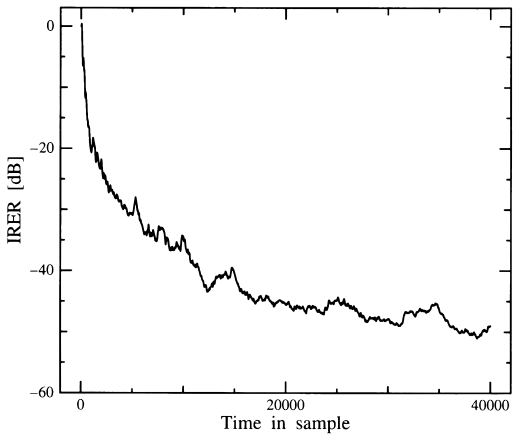

(c) IRER convergence characteristics.

Fig. 10 Simulation example of the proposed method ($L = 53$, $D = 50$, $N = 3$, $M = 4$).

By using the proposed technique, we can identify the impulse response of the dispersive region using only M adaptive weights in the frequency domain.

6.2 Comparison of the LMS Algorithm

We consider the comparison of the least mean square (LMS) algorithm and the proposed method assuming an echo cancellation. Figure 8 shows an echo canceler block diagram.

The unknown impulse response $h(n)$ is defined as

$$\begin{array}{ll} \text{Flat delay :} & h(0) \text{ to } h(D-1) \\ \text{Dispersive region :} & h(D) \text{ to } h(D+N-1) \\ \text{Residual delay :} & h(D+N) \text{ to } h(L-1), \end{array} \tag{16}$$

where $L = 400$, $N = 51$ and $D = 90$, 100, 155.

The dispersive response region of the echo path $h(k)$ is defined as [5]

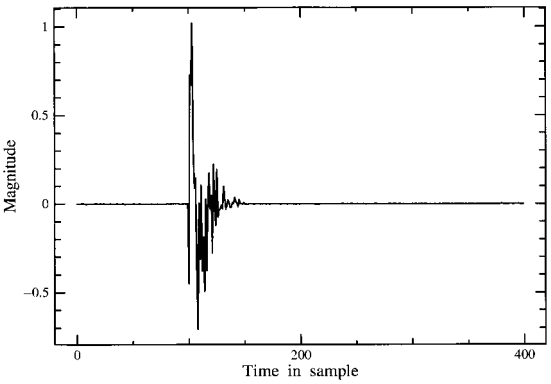

Fig. 11 Unknown impulse response ($D = 100$).

$$h(k) = \exp\{-0.1 \times (k - D)\} \cdot w(k) \quad (17)$$
$$k = D, D+1, \cdots, D+N-1.$$

where $w(k)$ is Gaussian noise of zero mean with unit variance. The flat delay and residual delay region consist of Gaussian noise of zero mean with variance of 10^{-6}. These Gaussian noise are uncorrelated with together. Figure 11 shows the unknown impulse response in the case of $D = 100$.

The input signal $x(n)$ is 40000 points colored signal which generated by the coloring filter $C(z)$ with Gaussian noise of zero mean with unit variance.

$$C(z) = \frac{0.1}{1 - 0.9z^{-1}} \quad (18)$$

All simulation examples are done with 100 trial. $g(n)$ represent additive Gaussian noise of zero mean with variance of 10^{-3}.

The all Gaussian noise are uncorrelated with among them. Another conditions are summarized as follows.

[Proposed algorithm]
FFT size: $M = 64$
Forgetting constant: $\alpha = \lambda = 0.9999$

[Full tap LMS]
Tap lenghth: $K = 400$
Number of adaptive weights: $N_L = 400$
Step size: $\mu = 0.005$

[Sparse tap LMS]
Tap lenghth: $K = 400$
Number of adaptive weights: $N_L = 64$
Number of Fixed delay: $D_L = 100$
Step size: $\mu = 0.04$

In the LMS algorithm, step size μ is chosen as fastest and stable from the experimentation. In the full tap LMS algorithm, the adaptive filter has entire adaptive weights on their taps, whereas sparse tap algorithm only has N_L taps as shown in Fig. 2. In addition, the sparse tap LMS adaptive filter equipped with fixed delay $D_L = 100$ to concentrate the dispersive response region.

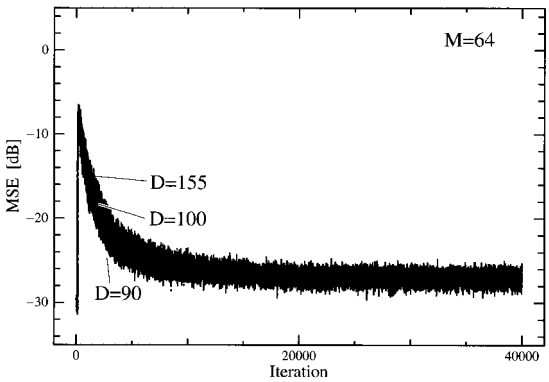

(a) Proposed ($M = 64$).

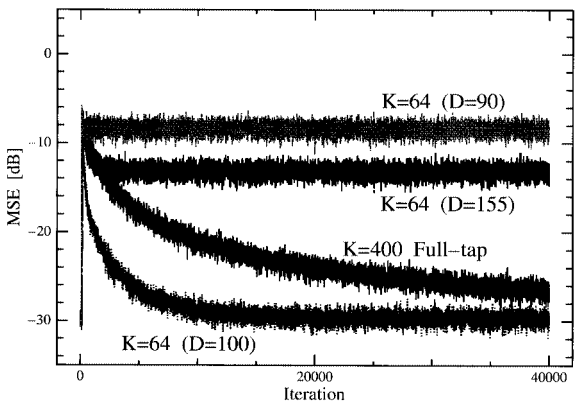

(b) LMS algorithm.

Fig. 12 MSE convergence characteristics.

Figures 12 (a) and (b) show MSE convergence of the proposed algorithm and LMS algorithms, respectively. The definition of the MSE is given by

$$\text{MSE} = 10 \log_{10} E[e^2(n)] \quad (19)$$

where n represents time index.

From Figs. 12 (a) and (b), the proposed algorithm as fast as the sparse tap LMS algorithm with fixed delay $D = D_L = 100$. Regardless of the value of D, proposed algorithm shows robustness as shown in Fig. 12 (a).

The sparse tap LMS algorithm with fixed delay converges faster than the full tap LMS algorithm. On the other hand, if the fixed delay D_L does not agree with the delay D, the residual error becomes quite large in the case of $D = 90$ and $D = 155$. By applying the tap selection algorithm [5]–[7] to the sparse tap adaptive filter enables significantly improvement of the convergence property. However, the penalty of the miss adjustment in the tap selection algorithm is not always small.

7. Conclusion

In this paper, we proposed the use of the frequency domain adaptive algorithm based on the frequency domain sampling theorem, to estimate impulse response with a flat delay and dispersive region. The proposed technique enables efficient identification of the impulse response with a flat delay and dispersive region.

Since the proposed technique can evaluate the subband signal in equally spaced discrete frequency points, regardless of the flat delay with length D, it can reduce both the number of adaptive weights and the complexity of the flat delay estimation.

In addition, the flat delay estimation and the impulse response estimation of the dispersive region can be performed independently. Thus the impulse response estimation accuracy is not disturbed by the changing of the flat delay D.

References

[1] D.L. Duttweiler, "A twelve-channel digital echo canceller," IEEE Trans. Commun., vol.COM-26, pp.647–653, May 1978.
[2] D.L. Duttweiler, "Subsampling to estimate delay with application to echo cancelling," IEEE Trans. Acoust., Speech & Signal Process., vol.ASSP-31, pp.1090–1099, Oct. 1983.
[3] D.M. Etter and Y.F. Cheng, "System modeling using an adaptive delay filter," IEEE Trans. Circuits & Syst., vol.CAS34, no.7, pp.770–774, July 1987.
[4] S. Kawamura and M. Hatori, "A tap selection algorithm for adaptive filters," Proc. IEEE International Conference on ICASSP'86, pp.2979–2982, April 1986.
[5] A. Sugiyama and S. Ikeda, "A fast convergence algorithm for adaptive FIR filters with sparse taps," IEICE Trans. Fundamentals, vol.E77-A, no.4, pp.681–687, April 1994.
[6] A. Sugiyama, H. Sato, A. Hirano, and S. Ikeda, "A fast convergence algorithm for adaptive FIR filters under computational constraint for adaptive tap-position control," IEEE Trans. Circuits & Syst.II, vol.43, no.9, pp.629–636, Sept. 1996.
[7] A. Sugiyama, K. Anzai, H. Sato, and A. Hirano, "Cancellation of multiple echoes by multiple autonomic and distributed echo canceller units," IEICE Trans. Fundamentals, vol.E81-A, no.11, pp.2361–2369, Nov. 1998.
[8] Y. Yamada, H. Ochi, and H. Kiya, "A subband adaptive filter allowing maximally decimation," IEEE J. Select. Areas Commun, vol.12, no.9, pp.1548–1552, Dec. 1994.
[9] A. Antoniou, Digital Filters: Analysis, Design, and Applications, 2nd ed. McGraw Hill, 1993.
[10] H. Ochi, S. Kinjo, and H. Kiya, "A new frequency domain adaptive filters based on the frequency domain sampling theorem," Proc. 11th European Conference, Davos, Switzerland, Part 1, pp.109–114, Sept. 1993.
[11] S. Kinjo, Y. Yamada, and H. Ochi, "A new cost function for system identification utilizing an alias free parallel adaptive filter," IEICE Trans. Fundamentals, vol.E77-A, no.9, pp.1426–1431, Sept. 1994.
[12] U. Iyer, M. Nayeri, and H. Ochi, "Polyphase based adaptive structure for adaptive filtering and tracking," IEEE Trans. Circuits & Syst.II, vol.43, no.3, pp.220–233, March 1996.
[13] H. Kiya and S. Yamaguchi, "FSF (Frequency Sampling Filter) bank for adaptive system identification," Proc. IEEE International Conference on ICASSP'92, San Francisco, March 1992.
[14] H. Kiya, H. Yamazaki, and Y. Yamada, "A design method of filter banks with alias-free characteristics at equally spaced frequency points," IEICE Trans. Fundamentals, vol.J77-A, no.12, pp.1632–1639, Dec. 1994.

Yoji Yamada was born in Ishikawa, Japan, on March 22, 1965. He received his B.E. and M.E. degrees in electrical engineering from Nagaoka University of Technology, Niigata, Japan, in 1987 and 1989, respectively. From 1989 to 1990, he worked at the Research Laboratory, Anritsu Corporation as a researcher. In 1990, he joined Ishikawa National College of Technology, where he is currently a lecturer in the department of Electronics and Information Engineering. His research interests include in digital signal processing, multirate systems and adaptive filtering. He is a member of the IEEE CAS and Signal Processing societies.

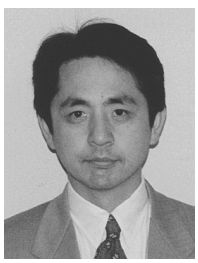

Hitoshi Kiya was born in Yamagata, Japan, on November 16, 1957. He received his B.E. and M.E. degrees in electrical engineering from Nagaoka University of Technology, Niigata, Japan, and his D.E. degree in electrical engineering from Tokyo Metropolitan University, Tokyo, Japan, in 1980, 1982 and 1987, respectively. In 1982, he joined Tokyo Metropolitan University, where he is currently an Associate Professor in the department of Electrical Engineering, Graduate School of Engineering. He was a visiting researcher at the University of Sydney in Australia from Oct. 1995 to Mar. 1996. His research interests include in digital signal processing, multirate systems, adaptive filtering, image processing and efficient algorithms for VLSI implementation. Dr. Kiya is a Member of the IEEE, the Image Electronics Engineers of Japan and the Institute of Television Engineers of Japan. He is an Associate Editor of IEEE Transactions on Signal Processing of IEEE.

Noriyoshi Kambayashi graduated in 1963 from the Department of Communication Engineering, Faculty of Engineering, Shinshu University. He has a Doctor of Engineering degree. In 1967, he was a research associate in the Department of Electrophysics, Faculty of Engineering, Tokyo Institute of Technology, an Associate Professor in 1978 in the Department of Electrical Engineering, Faculty of Engineering, Nagaoka University of Technology, and is presently a Professor. He is engaged in research on electronic circuits and digital signal processing theory together with there applications. He is the author of "Theory and Design of Filters" and "Basic Circuits Engineering," among other books.